---

**Article:**
Dickinson, Elizabeth orcid.org/0000-0001-8961-3230, Arnold, John R. P. and Fisher, Julie (2017) Determination of glucose exchange rates and permeability of erythrocyte membrane in preeclampsia and subsequent oxidative stress-related protein damage using dynamic-19F-NMR. JOURNAL OF BIOMOLECULAR NMR. pp. 1-12. ISSN 0925-2738

https://doi.org/10.1007/s10858-017-0092-y

---

J Biomol NMR
DOI 10.1007/s10858-017-0092-y

ARTICLE

# Determination of glucose exchange rates and permeability of erythrocyte membrane in preeclampsia and subsequent oxidative stress-related protein damage using dynamic-$^{19}$F-NMR

**Elizabeth Dickinson**[1] · **John R. P. Arnold**[2] · **Julie Fisher**[3]

Received: 21 December 2016 / Accepted: 27 January 2017


**Abstract** The cause of the pregnancy condition preeclampsia (PE) is thought to be endothelial dysfunction caused by oxidative stress. As abnormal glucose tolerance has also been associated with PE, we use a fluorinated-mimic of this metabolite to establish whether any oxidative damage to lipids and proteins in the erythrocyte membrane has increased cell membrane permeability. Data were acquired using $^{19}$F Dynamic-NMR (DNMR) to measure exchange of 3-fluoro-3-deoxyglucose (3-FDG) across the membrane of erythrocytes from 10 pregnant women (5 healthy control women, and 5 from women suffering from PE). Magnetisation transfer was measured using the 1D selective inversion and 2D EXSY pulse sequences, over a range of time delays. Integrated intensities from these experiments were used in matrix diagonalisation to estimate the values of the rate constants of exchange and membrane permeability. No significant differences were observed for the rate of exchange of 3-FDG and membrane permeability between healthy pregnant women and those suffering from PE, leading us to conclude that no oxidative damage had occurred at this carrier-protein site in the membrane.

**Keywords** NMR · Dynamic · Exchange · Membrane · Preeclampsia · Oxidative stress

## Introduction

Preeclampsia (PE) is a human-specific hypertensive disorder of pregnancy which manifests itself after 20 weeks of gestation, developing in almost 10% of pregnancies (El Hassan et al. 2015; Kumru et al. 2006). The cause of PE is still not fully understood, though it is a major cause of maternal and foetal morbidity and mortality. PE affects the mother by vascular endothelial dysfunction and causes intrauterine growth restriction of the foetus (Hubel 1999; Poston et al. 2006). Delivery of the baby is the only method of reversing the syndrome.

Numerous etiologies have been asscociated with PE, though the attack of reactive oxygen species (ROS), and oxidative stress, is thought to be the most important factor contributing to the pathogenesis of PE, causing uncontrolled lipid peroxidation, protein modification and changes to cell membrane structure (Raijmakers et al. 2008; Ethordevic et al. 2008; Adiga et al. 2007; Mohan and Venkataramana 2007; Shoji et al. 2008; Shoji and Koletzko 2007). It has been suggested that polyunsaturated fatty acids are attacked by ROS and converted into lipid hydroperoxides as the initial factor leading to vascular endothelial dysfunction in PE (Howlander et al. 2007; Kaur et al. 2008; Hubel et al. 1989; Davidge et al. 1992; Mehendale et al. 2008; Patil et al. 2007).

Products of lipid peroxidation have the ability to cause further oxidative damage by attacking proteins present in the cells and tissue, which in turn causes lysis of erythrocytes (Salvi et al. 2001; Negre-Salvayre et al. 2008; Davies 1987; Esterbaur et al. 1991). Oxidative damage to

**Electronic supplementary material** The online version of this article (doi:10.1007/s10858-017-0092-y) contains supplementary material, which is available to authorized users.

✉ Elizabeth Dickinson
elizabeth.dickinson@york.ac.uk

[1] Department of Chemistry, University of York, Heslington, York, UK

[2] Selby College, Abbot's Road, Selby, North Yorkshire YO8 8AT, UK

[3] School of Chemistry, University of Leeds, Leeds, UK

Published online: 21 February 2017

membrane proteins can also occur by direct free radical attack—such protein modifications can cause structural changes and may also result in detrimental changes in their function, affecting activity of enzymes, receptors or membrane transporters (Roche et al. 2008; Jones 2008; Stadtman 1993).

Abnormal glucose tolerance has also been implicated as a risk factor for PE (Joffe et al. 1998; Parra-Cordero et al. 2014). Glucose enters and leaves the red blood cell by passive transport via an intrinsic protein, GLUT1, so that the facilitated diffusion of this species in and out of erythrocytes is in dynamic equilibrium (May 1998; Gabel et al. 1997; O'Connell et al. 1994; Potts et al. 1990; Potts and Kuchel 1992; London and Gabel 1995). However, any damage to membrane proteins or lipids due to oxidative stress may cause changes in their conformation, which could affect the rate at which the diffusion of species across the membrane occurs. We have demonstrated previously that NMR is capable of identifying metabolomic differences in the blood of healthy pregnant women and those suffering from PE (Turner et al. 2007, 2008, 2009). We therefore used NMR spectroscopy to investigate the hypothesis that a difference in glucose exchange rate and cell membrane permeability will be observed between healthy pregnant women and those suffering from PE.

NMR exchange experiments allow processes to be investigated under dynamic equilibrium (Perrin and Dwyer 1999; Perrin and Engler 1990; Perrin and Gipe 1984; Robinson et al. 1985). This is achieved by monitoring the transfer of longitudinal magnetisation during a delay in the NMR pulse sequence applied (Grassi et al. 1986; McConnell 1958; Forsén and Hoffman 1963; Muhandiram and McClung 1987). In the application of dynamic NMR (D-NMR) to the study of exchange in erythrocytes from pregnant women, both one dimensional and two-dimensional spectra have been recorded to detect exchange pathways and determine rates of exchange and relaxation of species. By applying both experiments, the results obtained for each can be compared and confirmed, to ensure that the estimates of the values of the rate constants obtained are reliable. As demonstrated previously, 2D methods provide a qualitative map of the exchange process and are tolerant to small differences in chemical shift between the peaks involved in exchange (Johnston et al. 1986; Macura and Ernst 1980); the 1D methods provide faster data acquisition and analysis, especially for two-site systems, as long as the exchange network is known (Perrin and Engler 1990; Robinson et al. 1985; Engler et al. 1988). The integrated intensities obtained from the 1D and 2D experiments can then be used to estimate the values of the first order rate constants of exchange, and establish if oxidative damage has indeed compromised the erythrocyte membrane (Gabel et al. 1997; Perrin and Dwyer 1999; Perrin and Gipe 1984). Whilst the processes of exchange and the nuclear Overhauser effect are different, both rely on the transfer of longitudinal magnetisation, which is why the same pulse sequence can be applied.

Several one-dimensional experiments exist based on the NOESY pulse sequence, which can be employed to measure the transfer of magnetisation (Robinson et al. 1985; Bellon et al. 1987; Engler et al. 1988; Bulliman et al. 1989; Perrin and Engler 1990). Whilst the "Overdetermined" 1D EXSY pulse sequence of Bulliman et al. (1989) has also been used to study erythrocytes (Potts and Kuchel 1992), the more complex matrix diagonalisation methods are different to those employed in most other exchange applications. Selective inversion was the 1D method of choice in this investigation (Robinson et al. 1985). The exchange of species monitored by 2D spectroscopy was initially documented by Jeener et al. (1979), and has become invaluable in establishing the mechanisms of exchange (Perrin and Gipe 1984; Meier and Ernst 1979; Macura and Ernst 1980; Bremer et al. 1984; Johnston et al. 1986; Montelione and Wagner 1989). The principle is similar, as expected, to that for the selective inversion experiment and so should give comparable results for the elements of the rate matrix. Exchange occurs during the mixing time and in the 2D EXSY four peaks will be produced in the two-site case of cellular exchange i.e. two cross peaks and two diagonal peaks (Gabel et al. 1997; O'Connell et al. 1994; Kirk and Kuchel 1985; Potts et al. 1989). The volumes of all these peaks can then be used in matrix diagonalisation to estimate the values of the exchange rate and relaxation rate constants. A full explanation of the matrix diagonalization method has been included in the Appendix for completeness, as the procedure is not used nor fully described very often in the literature.

By estimating the values of the rate constants of cellular exchange, the measurement of the permeability of the erythrocyte membrane is possible. This will give information on the condition of the membrane with a higher permeability in PE providing an indication of oxidative stress or attack and compromise of the lipid bilayer by ROS.

The inward permeability is calculated from the inward rate constant, previously determined from the NMR data:

$$P_1 = \frac{V_e}{A}k_1 = \frac{MCV(1-Ht)}{A_{cell}(Ht)}k_1 \quad (1)$$

here $Ht$ is the haematocrit (or red blood cell count); $V_e$ is the extracellular volume (mL), calculated as $V_o(1\text{-}Ht)$, where $V_o$ is the NMR sample volume; $A$ is the total surface area of the cells, calculated from $(A_{cell}Ht)$/MCV, where $A_{cell} = 1.43\times10^{-6}$ cm$^2$ and MCV (mean cell volume) = 85 fL for erythrocytes in isotonic solution; $k_1$ = influx rate constant (Raftos et al. 1990; O'Connell et al. 1994; London and Gabel 1995; Chapman and Kuchel 1990).

Similarly, the outward permeability can be calculated using the efflux rate constant:

$$P_{-1} = \frac{V_i}{A} k_{-1} = \frac{MCVf_w}{A_{cell}} k_{-1} \quad (2)$$

where $f_w$ is the fraction of red cell volume which is accessible to solutes, and $k_{-1}$ is the efflux rate constant (Raftos et al. 1990; O'Connell et al. 1994; London and Gabel 1995). It is clear from Eq. (2) that the outward permeability is independent of haematocrit.

## Materials and methods

### Patient selection and sample preparation

Women chosen for this part of the study were all beyond 20 weeks of gestation and were attending The Leeds Teaching Hospitals NHS Trust, Leeds, UK. The women were of any ethnicity and were not all in their first pregnancy. The PE group exhibited fully established PE, diagnosed according to the criteria of American College of Obstetrics and Gynecologists (ACOG) i.e., a rise in blood pressure after 20 weeks gestation to >140/90 mm Hg on two or more occasions 6 h apart in a previously normotensive woman, combined with proteinuria (Davey and MacGillivray 1988). Proteinuria was defined as protein dipstick >1 + on two or more midstream urine samples, or a 24 h urine excretion of >0.3 g protein, in the absence of a urinary tract infection (Harsem et al. 2006). Healthy control women were generally from later in pregnancy, i.e. >30 weeks, to ensure that they remained healthy controls and did not develop PE weeks after sample collection. Venous blood was collected in heparinized (lithium salt) anticoagulant tubes. All fresh whole blood was centrifuged for 6 min at 3000 g and 4 °C, before removing and discarding the plasma and buffy coat. The same conditions were used in all subsequent washings of erythrocytes. For the transport of 3FDG, a saline buffer solution was prepared containing 132 mM NaCl, 15 mM Tris-HEPES (pH 7.4), 5 mM ascorbic acid and 10 mM 3FDG (O'Connell et al. 1994; Pallotta et al. 2014). Erythrocytes (still in the anticoagulant tube) were washed with the saline buffer solution in $D_2O$ containing the fluorinated glucose, using approximately three times the volume of the RBCs. The tube was inverted three times to mix the solution and RBCs before repeating centrifugation, and removing and discarding the wash solution. This washing procedure was repeated three times. After washing, carbon monoxide gas was bubbled through the cells for approximately 30 s with gentle stirring to remove deoxyhaemoglobin and paramagnetic $O_2$ from the sample (O'Connell et al. 1994). Finally, the haematocrit of the sample was measured in duplicate using heparinised capillary tubes, and spun at approximately 1300 g for 5 min using a Haematospin 1300 (Hawsley, Lancing, Sussex, UK). It was assumed that 0.717 of the intracellular volume was accessible to the 3FG molecules (Potts and Kuchel 1992).

The RBCs were incubated at 37 °C for 1 h, before transferring 700 µl of the RBCs/glucose solution to an NMR tube for analysis.

### 1D $^{19}$F spectra fluorinated glucose in $D_2O$

The 1D $^{19}$F-NMR FID of 5 mM 3-fluoro-3-deoxyglucose (3FDG) in $D_2O$ was acquired at 470.34 MHz and at 37 °C into 65,536 data points, using a relaxation delay of 5 s, a pulse duration of 10 µs, over 4 transients, at a temperature of 20 °C. An exponential line broadening of 1 Hz was applied to the FID, prior to zero filling to 131,072 points, followed by Fourier transformation. Resultant spectra were phased and baseline corrected using Vnmr 6.1 C (Varian Inc., Palo Alto, California, USA).

### 1D $^{19}$F spectra of RBCs and fluorinated glucose, with and without proton decoupling

Two one dimensional spectra were acquired of the RBCs and fluorinated glucose at 470.34 MHz and at 37°C, where broadband proton decoupling was applied in the second experiment. This allowed the $^{19}$F intracellular and extracellular resonances to be resolved without the complication of the geminal $^1$H-$^{19}$F coupling (Gabel et al. 1997). For both experiments, an interpulse relaxation delay of 8 s was used, a delay which was longer than $5T_1$ (O'Connell et al. 1994). The $^{19}$F 90° pulse duration was determined for each new sample though was often 17 µs. The coupling constant measured in the first 1D spectrum was used in the calibration of the $^1$H 90° pulse duration for the proton decoupling in the second experiment, during which WALTZ decoupling was applied for the duration of the pulse and acquisition. 128 transients were collected into 16,384 data points for each spectrum, with a spectral width of 10,000 Hz. An exponential line broadening of 1 Hz was applied to each of the FIDs, prior to zero filling to 32,768 points, followed by Fourier transformation. Resultant spectra were phased, baseline corrected and integrated using Vnmr 6.1 C (Varian Inc., Palo Alto, California, USA). Manual integration was repeated and the mean average taken to minimise errors.

### Selective inversion

One dimensional $^{19}$F magnetization transfer experiments were performed on RBCs and fluorinated glucose at 470.34 MHz and at 37°C using the selective inversion method (O'Connell et al. 1994; Gabel et al. 1997; Robinson et al. 1985). Two series of experiments were performed

for each anomer, using the 1D NOESY pulse sequence [RD–90°$_x$–$t_1$–90°$_x$–$t_m$–90°$_x$–acq], where either the intracellular or the extracellular peak was selectively inverted by setting the transmitter offset to the frequency of the resonance to be inverted. RD represents a relaxation delay of 8 s, a delay which was longer than $5T_1$ (O'Connell et al. 1994). The delay $t_1 = 1/(2|\nu_i\text{-}\nu_e|)$, where $\nu_i$ and $\nu_e$ are the frequencies of the intracellular and extracellular peaks respectively. The mixing time $t_m$ was arrayed at delays of 0.001 (nominal zero), 0.05, 0.075, 0.10, 0.15, 0.30 and 0.45 s. After calibration of the $^1$H 90° pulse duration, broadband proton decoupling was applied using WALTZ decoupling during the final pulse and acquisition. The $^{19}$F 90° pulse duration used in the initial one dimensional experiments was applied (often 17 μs). 128 transients were collected into 16,384 data points for each spectrum, with a spectral width of 10,000 Hz. Again, exponential line broadening of 1 Hz was applied to each of the FIDs, prior to zero filling to 32,768 points, followed by Fourier transformation. Resultant spectra were phased, baseline corrected and integrated using Vnmr 6.1 C (Varian Inc., Palo Alto, California, USA). Manual integration was repeated and the mean average taken to minimise errors.

### 2D EXSY

Four two dimensional magnetization transfer experiments were performed on the RBC and fluorinated glucose samples at 470.34 MHz and at 37°C, using the broadband proton decoupled 2D NOESY pulse sequence [RD–90°$_x$–$t_1$–90°$_x$–$t_m$–90°$_x$–acq] (Gabel et al. 1997; Macura and Ernst 1980; Johnston et al. 1986). Each experiment had a different mixing time, $t_m$, of either 0, 200, 400 or 600 ms. In all four experiments, 8 transients were collected into 4,096 data points in the directly detected dimension and 64 points in the second dimension, with a spectral width of 10,000 Hz. The same relaxation delay as in the 1D experiments was used (8 s), as well as the same previously calibrated $^{19}$F and $^1$H (for decoupling) pulse widths. Proton decoupling was provided in the directly detected dimension by application of WALTZ decoupling during the final pulse and acquisition. An exponential line broadening of 2 Hz was applied in both dimensions to each FID (O'Connell et al. 1994), prior to zero filling the second dimension to 2048 points, followed by Fourier transformation. Resultant spectra were phased and baseline corrected using Vnmr 6.1C (Varian Inc., Palo Alto, California, USA). Each spectrum was integrated using Lorentzian Fitting mode in the software Sparky 3.114 (T. D. Goddard and D. G. Kneller, SPARKY 3, University of California, San Francisco, USA), where peaks within a contour boundary were grouped, and where the data that were used were above the lowest contour.

### Matrix diagonalisation of integrated intensities

Integrated peak data from the 1D and 2D magnetization transfer experiments were analysed by matrix diagonalization using the software Maple 11 (Maplesoft, Waterloo Maple Inc, Waterloo, Ontario, Canada). Plots of the linearised matrix data were produced in Microsoft Excel (Microsoft Corporation, Redmond, WA USA), where the gradients of the lines in the plots were equal to elements of the relaxation matrix.

### Statistical analysis

After tests of normality had been performed, comparison of mean values (of integrated peaks, or rates of exchange) were performed, between the PE group and control group, using the *t* test or Mann–Whitney test in SPSS 13.0 software (SPSS Inc., Chicago, Illinois, USA). All *p* values were adjusted for multiple comparisons using false discovery rate in the software R 2.4.1 (R Foundation for Statistical Computing, Vienna, Austria), and values of $<0.05$ were regarded as statistically significant.

## Results

1D $^{19}$F spectra of 3FDG and washed erythrocytes are shown in Figs. 1 and 2 respectively, as well as examples of the 1D Selective Inversion (Fig. 3) and 2D EXSY (Fig. 4) magnetisation transfer experiments. Figure 3 shows the 2D EXSY spectrum of red blood cells washed with exchanging 3FDG. It is clear that mutarotation between anomers is too slow to occur on the timescale of the experiment, as no chemical exchange peaks are present between the β- and α-anomer. This allowed a simplification of the matrix diagonalisation methods; each anomer was treated as a separate probe, therefore producing 2, 2×2 rate matrices, rather than 1, 4×4 matrix (O'Connell et al. 1994; Gabel et al. 1997; Macura and Ernst 1980; Johnston et al. 1986). An example of a plot of the linearised data from the exchange equation is shown in Fig. 5. The mean average elements of the rate matrix, estimated from the magnetisation transfer experiments, and the calculated permeabilities for each anomer are shown in Table 1.

When testing the hypothesis that differences would occur between the elements of the rate matrix of women with PE and that of healthy control pregnant women, it was found that no significant differences were observed for any element of the rate matrix, for either glucose anomer. We therefore conclude that the rate of carrier-mediated exchange of fluorinated glucose is the same for women suffering from PE as that of healthy pregnant women. In turn, the membrane of an erythrocyte from a woman suffering

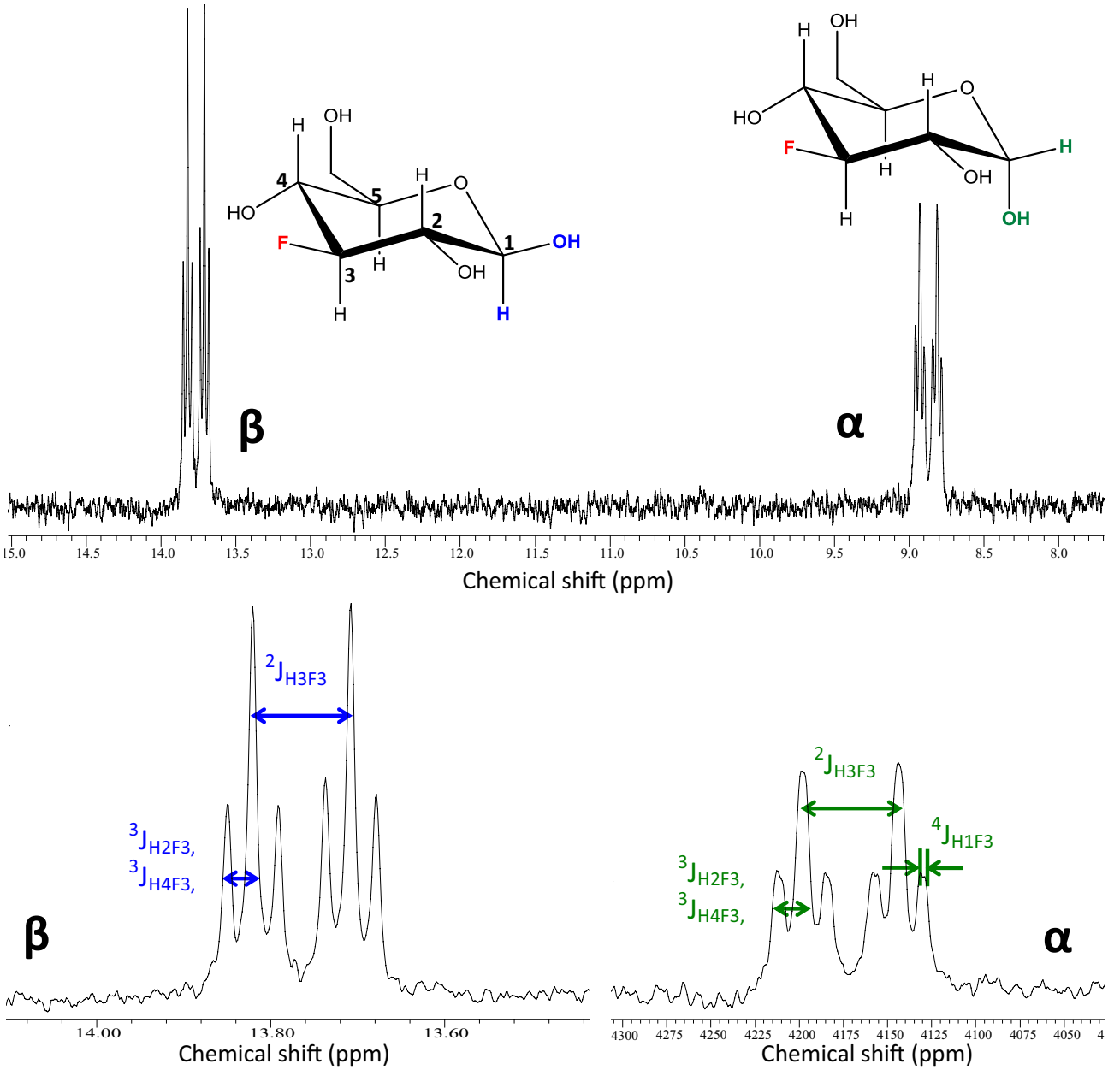


**Fig. 1** $^{19}$F NMR spectrum and structure of 3FDG in $D_2O$, at 470.34 MHz and at 37°C

from PE is no more or less permeable to 3FDG than that of erythrocytes from healthy pregnant women.

When testing the hypothesis that no differences would be identified between the elements of the rate matrix from the 1D Selective Inversion and that of the 2D EXSY experiments, significant differences were observed for the sum of the longitudinal relation rate constant of the intracellular peak and efflux rate constant i.e. $R_{11}$, $\frac{1}{T_{1_i}} + k_{io}$, ($p = 0.008$ for PE samples and 0.016 for control samples), and for both anomers of glucose (see Suppl Mat). Similarly, significant differences were found between the sum of the longitudinal relaxation rate constant of the extracellular peak and the influx rate constant ($R_{22}$,$\frac{1}{T_{1_o}} + k_{oi}$), determined using the 1D Selective Inversion, and that of the 2D EXSY, for the β-anomer only ($p = 0.016$). No other significant differences were observed between the results of the 1D and 2D experiments and the subsequently calculated permeabilities.

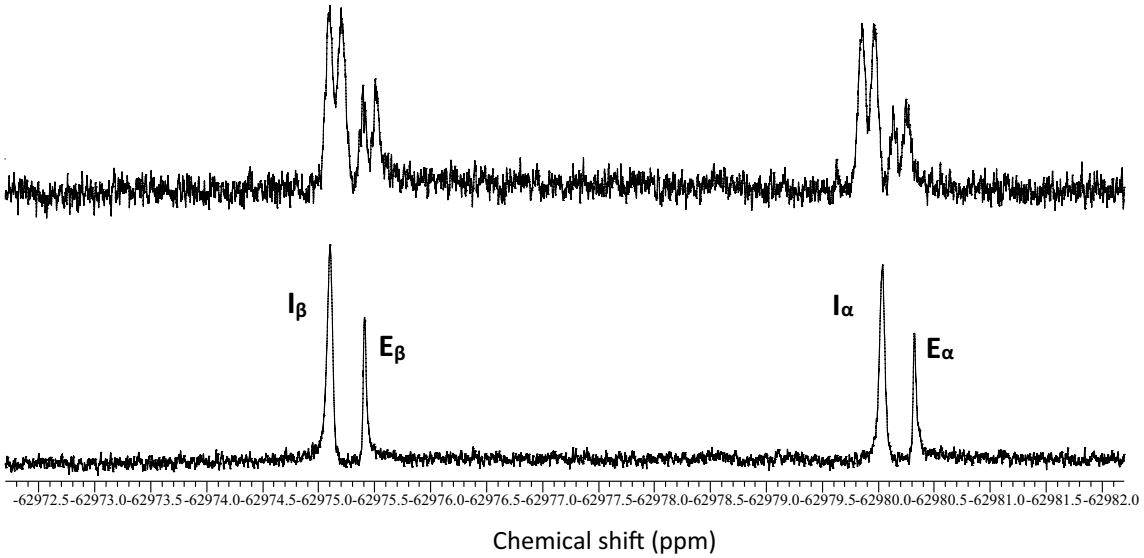


**Fig. 2** Spectra of erythrocytes washed with 3FDG solution (buffered with Tris-HEPES) where the bottom spectrum is broadband proton decoupled; I is intracellular 3-FDG and E is extracellular 3FDG (Ht = 79%)

## Discussion

The NMR investigation into exchange across the erythrocyte membrane was successful in estimating the values of the rates of exchange of a mimic of a natural product, and has been useful in investigating the effect of preeclampsia on the intrinsic protein GLUT1 involved in this facilitated diffusion.

For comparison of rates of exchange and permeabilities of membranes, the efflux rate constant $k_{io}$ and outward permeability $P_{io}$ are the most reliable parameters (Kirk and Kuchel 1986; O'Connell et al. 1994; Kuchel et al. 1987). The efflux rate constant is independent of haematocrit. Once inside the cells, the rate at which a molecule leaves a cell will not depend on the total number of cells in the sample outside the membrane. Analogous to this, the outward permeability is calculated from the efflux rate constant, and is therefore not dependent on haematocrit. The mean efflux rate constants of $2.284 \pm 0.695$ and $2.200 \pm 0.421$ $s^{-1}$ for the α- and β-anomers of 3FDG respectively are comparable to those found previously in the literature as well as supporting anomeric preference for α-anomer (Kuchel et al. 1987; Potts and Kuchel 1992; London and Gabel 1995). This slight anomeric preference was explained by London and Gabel (1995), who showed that the α-anomer preferentially binds to the carrier on the inside of the membrane, due to the conformation of the carrier at that time inside the cell. After transportation, the conformation of this carrier changes outside the membrane, preferentially binding β-glucose. The higher rate obtained in this investigation into PE could be attributed to pregnancy in general as the permeability of erythrocytes may be affected by pregnancy. However it is not possible to confirm this without performing the same experiments on an equivalent number of non-pregnant controls.

No significant differences between the 1D Selective Inversion and the 2D EXSY for both the efflux rate constant and the outward permeability suggests that the results obtained are reliable and the methods robust. The only significant differences observed between the 1D and 2D data were in the elements of the rate matrix which are dependent on haematocrit. $R_{11}$ includes the longitudinal relaxation rate of the broad intracellular peak $\frac{1}{T_{1_i}}$, whilst $R_{22}$ includes the influx rate constant $k_{oi}$ (see Suppl Mat). This difference can therefore be attributed to the estimation of peak volume and peak fitting in the 2D data due to the broadness of the intracellular peak, which is why previous studies favoured the 1D methods over 2D for simple two-site exchange (Perrin and Dwyer 1999; Engler et al. 1988; Robinson et al. 1985).

The substitution of a hydroxyl group for a fluorine atom on a glucose molecule does not seem to have an adverse effect on its exchange through the erythrocyte membrane. The exchange of 3FDG using the same protein as glucose has been demonstrated by Riley and Taylor (1973) who found that dilute solutions of glucose inhibited the transport of 3FDG. It has been suggested that the affinity of 3FDG for the binding site of the carrier is marginally higher, though not significantly so, than that of glucose itself, due to the F atom being directly involved in the hydrogen bonding in the binding site, mimicking that of the OH group of glucose (Riley and Taylor 1973; O'Connell et al. 1994). It is this hydrogen bonding which causes the difference in chemical shift

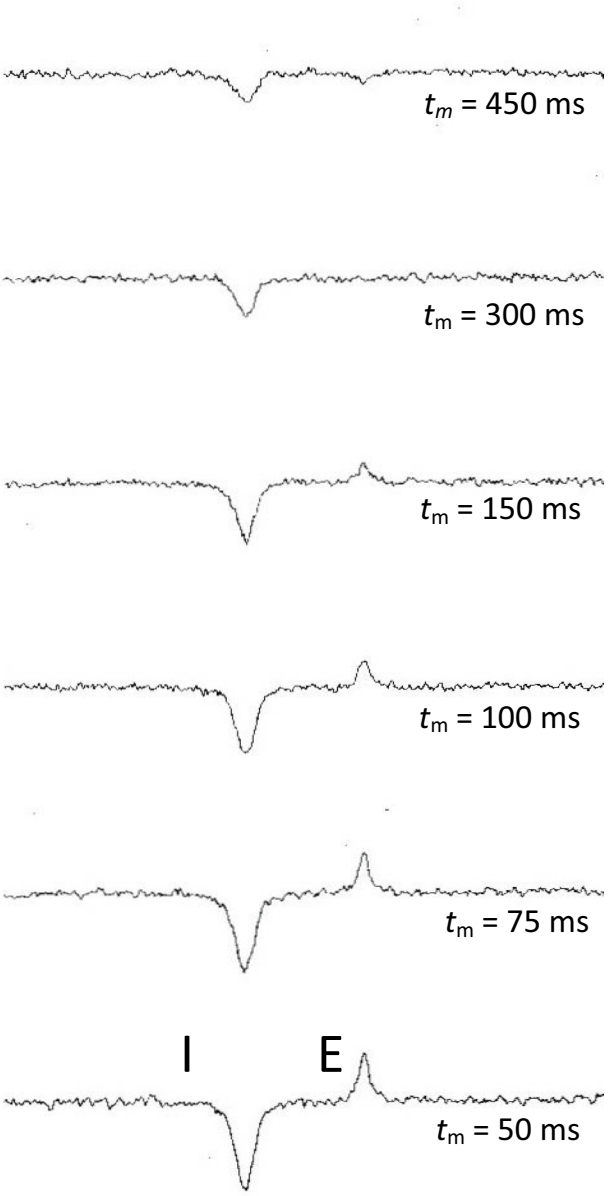


**Fig. 3** Expansions of the signals for the β-anomer of 3FDG, in exchange across the erythrocyte membrane, from the $^{19}$F-NMR 1D Selective Inversion spectra, acquired over a range of mixing times, $t_m$ (Ht = 79%)

between the intracellular and the extracellular populations. The intracellular hydrogen bonding will be different to that outside the cell as a result of the extent of the interactions present due to compartmentalisation and high protein concentration. The position of the fluorine atom on the hexose ring will also affect the extent of interactions. Preliminary investigations measuring the exchange of 2FDG clearly demonstrated this (see Suppl Mat). By increasing the osmolality of the wash solutions, the cellular volume is reduced, ensuring that the cytosol is isotonic with the extracellular medium, thus leading to a change in the intracellular interactions, and therefore a change in the chemical shift and broadness of the peak (Kirk and Kuchel 1985, 1988; Xu et al. 1991).

These effects, and the sharing of protein carrier GLUT1 by 3FDG and D-glucose, makes this study particularly useful in attempting to determine the effect of PE on the protein content of the erythrocyte membrane. Clearly, no significant differences between permeability or efflux rate constant of 3FDG between PE patients and healthy pregnant women showed that PE did not affect this protein part of the membrane. This result does not, however, rule out damage to the membrane by ROS of oxidative stress in PE, and does not contradict the results from earlier investigations; this study simply confirms that PE did not affect this particular protein transporter in executing facilitated diffusion of glucose and its mimics.

## Conclusions

$^{19}$F-Dynamic NMR spectroscopy proved to be a successful technique in measuring the cellular exchange rate of analogues of endogenous metabolites—the results of both the 1D and 2D magnetisation transfer experiments suggest that preeclampsia does not have deleterious effects on the erythrocyte membrane protein involved in glucose exchange.

## Appendix

The 1D Selective Inversion experiment is performed over an array of mixing times, during which the labelled probe is transported across the cell membrane, allowing the nucleus of interest to precess at a different frequency to that at its previous location (Kuchel et al. 1988; Robinson et al. 1985; Gabel et al. 1997; O'Connell et al. 1994; London and Gabel 1995). The integrated intensities of the intracellular (I) and extracellular (E) peaks are measured for each mixing time throughout the range, whilst the intracellular peak is inverted. This procedure is repeated with the extracellular peak inverted. Additionally, it is necessary to ascertain the integrated intensities of both the I and E peak under equilibrium conditions (Bulliman et al. 1989; Perrin and Engler 1990). Once all integrated intensities have been obtained, matrices can be formed, based upon the Exchange Eq. (3):

$$\mathbf{M}_t = e^{-Rt}\mathbf{M}_0 \tag{3}$$

where

$$\mathbf{M}_t = \begin{bmatrix} A_{t_m} - A_{equi} \\ B_{t_m} - B_{equi} \end{bmatrix} \quad \mathbf{M}_0 = \begin{bmatrix} A_{t_m=0} - A_{equi} \\ B_{t_m=0} - B_{equi} \end{bmatrix} \tag{4}$$

Matrices of (4) are calculated from three matrices produced directly from the integrated intensities. These three

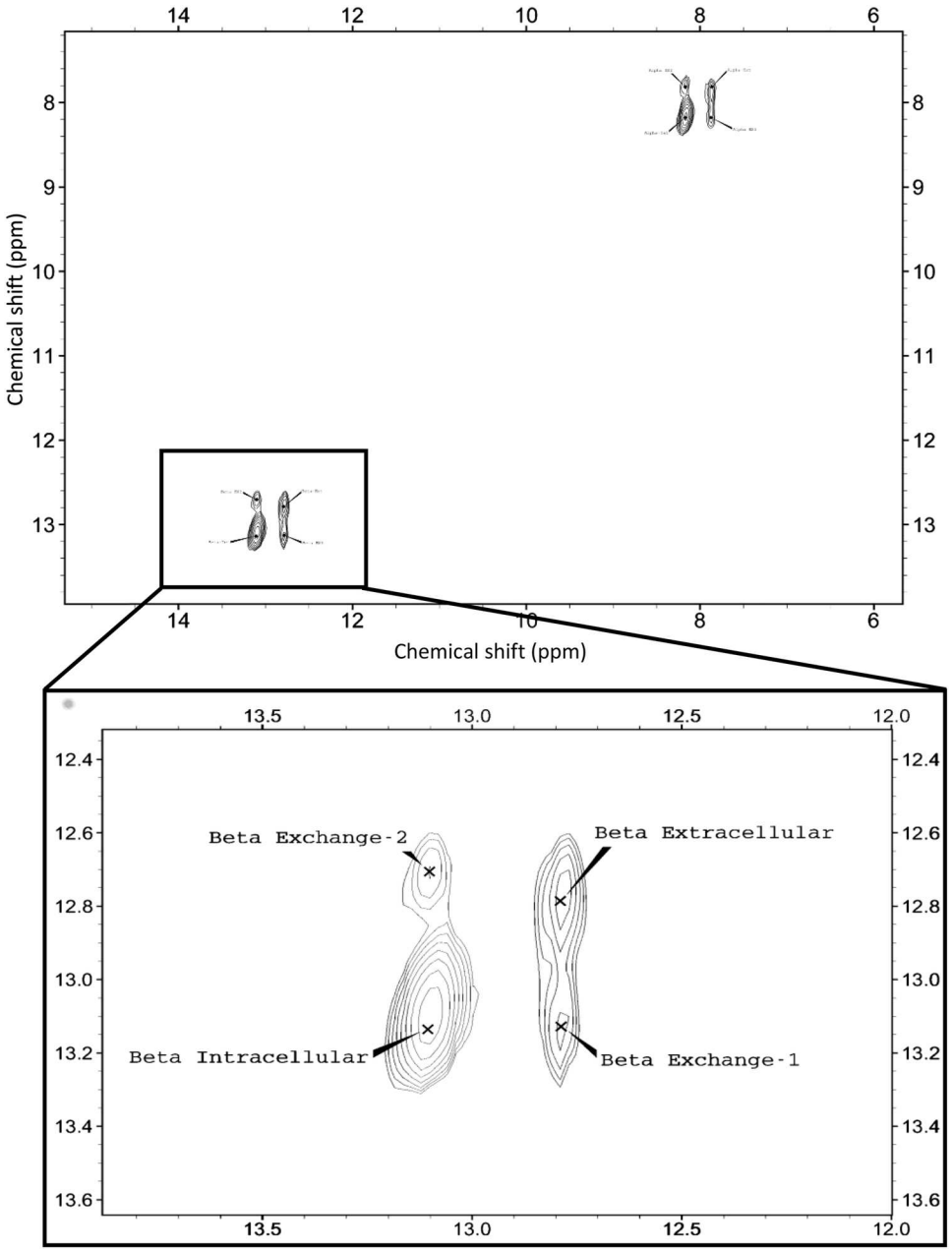


**Fig. 4** 2D EXSY $^{19}$F-NMR spectrum, with expansion of β-anomer peaks, of erythrocytes washed in 3FDG solution; no cross peaks between the anomers shows that mutarotation is slow on the timescale of the experiment (Ht = 79%)

matrices, $\mathbf{M}_{t_m}$, $\mathbf{M}_{t_m=0}$ and $\mathbf{M}_{\text{equilibrium}}$ are initially formed in the same way as the Matrix in (5):

$$\mathbf{M} = \begin{bmatrix} A_{\text{A inverted}} & A_{\text{B inverted}} \\ B_{\text{A inverted}} & B_{\text{B inverted}} \end{bmatrix} \tag{5}$$

where, for example, $A_{\text{A inverted}}$ is the integrated intensities of the resonance at site A, when this resonance is inverted. Matrices in (4) can be produced by simple subtraction. This process is repeated for each mixing time used in the range.

The Exchange Eq. (3) can then be linearised:

$$\mathbf{M}_t = e^{-\mathbf{R}t}\mathbf{M}_0 \rightarrow \ln\left(\mathbf{M}_t\mathbf{M}_0^{-1}\right) = -\mathbf{R}t \tag{6}$$

However, the difficulty of calculating the logarithm of a matrix is circumvented by using an alternative solution (7) where exponentials are eliminated:

$$\ln\left(\mathbf{M}_t\mathbf{M}_0^{-1}\right) = \mathbf{X}(\ln\Lambda)\mathbf{X}^{-1} = -\mathbf{R}t \tag{7}$$

Here $\mathbf{X}$ is the square matrix of eigenvectors of $(M_tM_0^{-1})$, $X^{-1}$ is its inverse, and ln Λ is the diagonal eigenvalue matrix (Jeener et al. 1979; Bremer et al. 1984; Johnston et al. 1986; Hernandez-Garcia et al. 2007; Szekely et al. 2006). This is formed as ln Λ = diag(ln λ), as shown in the Matrix of [8] (Johnston et al. 1986):

$$\ln\Lambda = \begin{bmatrix} \ln\lambda_1 & 0 \\ 0 & \ln\lambda_2 \end{bmatrix} \tag{8}$$

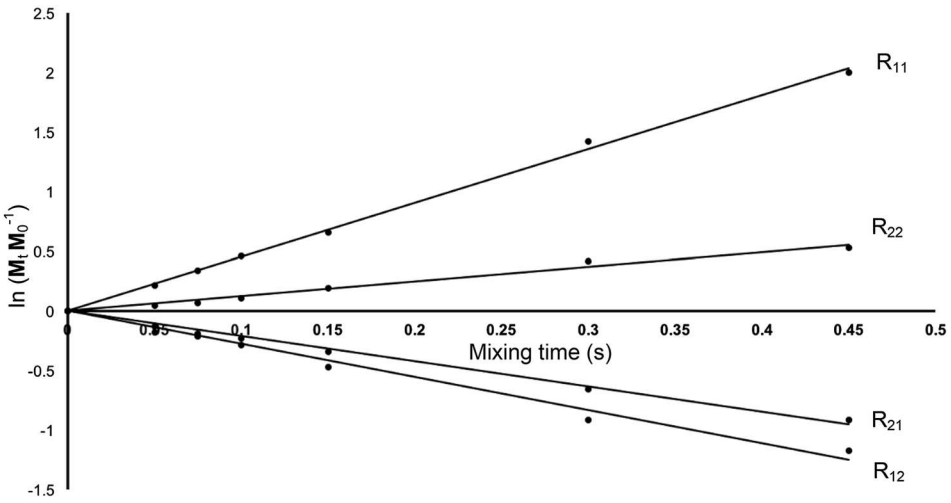


**Fig. 5** Plot of the linearised data from the exchange equation as function of mixing time (s), giving the elements of the rate matrix, R, for a control blood sample. $R_{11}$ ($\frac{1}{T_{1_i}} + k_{io}$)=4.52 $s^{-1}$ ($r^2$=1.00); $R_{12}$ ($k_{oi}$)=2.78 $s^{-1}$ ($r^2$=0.98); $R_{21}$($k_{io}$)=2.11 $s^{-1}$ ($r^2$=0.99); and $R_{22}$ ($\frac{1}{T_{1_o}} + k_{oi}$)=1.22 $s^{-1}$ ($r^2$=0.98)

**Table 1** Results of both 1D and 2D magnetisation transfer experiments on 3FDG exchange (errors are one standard deviation)

| Anomer | Element of rate matrix and permeabilities | | 1D Selective inversion | | | 2D EXSY | | |
|---|---|---|---|---|---|---|---|---|
| | | | PE, n=5 | CONTROL, n=5 | *p*-value | PE, n=5 | CONTROL, n=5 | *p*-value |
| β | $\frac{1}{T_{1_i}} + k_{io}$ ($s^{-1}$) | $R_{11}$ | 4.67±0.85 | 4.64±0.82 | 0.841 | 1.85±0.55 | 1.81±0.10 | 0.730 |
| | $k_{oi}$ ($s^{-1}$) | $R_{12}$ | 3.06±0.40 | 3.23±0.52 | 0.548 | 3.32±0.49 | 3.61±0.62 | 0.841 |
| | **$k_{io}$ ($s^{-1}$)** | **$R_{21}$** | **2.13±0.07** | **2.14±0.14** | **0.841** | **2.40±0.31** | **2.12±0.23** | **0.286** |
| | $\frac{1}{T_{1_o}} + k_{oi}$ ($s^{-1}$) | $R_{22}$ | 1.50±0.18 | 1.40±0.16 | 0.421 | 1.41±0.59 | 1.03±0.06 | 0.190 |
| | Inward permeability (cm $s^{-1}$) | | $3.85\pm0.56\times10^{-5}$ | $3.73\pm0.51\times10^{-5}$ | 1.000 | $4.15\pm0.54\times10^{-5}$ | $4.16\pm0.68\times10^{-5}$ | 1.000 |
| | Outward permeability (cm $s^{-1}$) | | $9.06\pm0.31\times10^{-5}$ | $9.13\pm0.59\times10^{-5}$ | 0.841 | $1.01\pm0.13\times10^{-4}$ | $9.25\pm0.94\times10^{-5}$ | 0.286 |
| | $\frac{P_{oi}}{P_{io}}$ | | 0.42±0.05 | 0.41±0.05 | 0.421 | 0.42±0.05 | 0.46±0.12 | 0.556 |
| α | $\frac{1}{T_{1_i}} + k_{io}$ ($s^{-1}$) | $R_{11}$ | 5.57±1.07 | 5.80±0.56 | 0.421 | 2.07±1.09 | 2.17±1.41 | 0.905 |
| | $k_{oi}$ ($s^{-1}$) | $R_{12}$ | 3.06±0.74 | 4.18±0.46 | 0.310 | 4.18±1.07 | 4.16±2.56 | 0.841 |
| | **$k_{io}$ ($s^{-1}$)** | **$R_{21}$** | **2.48±0.24** | **2.34±0.24** | **0.310** | **2.34±0.40** | **1.99±0.45** | **0.413** |
| | $\frac{1}{T_{1_o}} + k_{oi}$ ($s^{-1}$) | $R_{22}$ | 1.78±0.26 | 1.74±0.13 | 0.690 | 1.55±0.72 | 1.29±0.54 | 0.730 |
| | Inward permeability (cm $s^{-1}$) | | $4.52\pm0.87\times10^{-5}$ | $4.84\pm0.42\times10^{-5}$ | 0.841 | $5.23\pm2.03\times10^{-5}$ | $4.69\pm2.79\times10^{-5}$ | 1.000 |
| | Outward permeability (cm $s^{-1}$) | | $1.05\pm0.10\times10^{-4}$ | $9.96\pm1.02\times10^{-5}$ | 0.310 | $9.94\pm1.71\times10^{-5}$ | $8.49\pm1.95\times10^{-5}$ | 0.413 |
| | $\frac{P_{oi}}{P_{io}}$ | | 0.43±0.06 | 0.49±0.05 | 0.151 | 0.52±0.16 | 0.53±0.29 | 0.905 |

Bold values relate to the efflux rate constant, the most reliable parameter to estimate rate of cellular exchange and therefore subsequent membrane damage

These linearised data can then be plotted as a function of mixing time, as shown in Fig. 5. The gradients of the best-fit straight lines produced will give the elements of the square rate matrix R (Johnston et al. 1986; Engler et al. 1988; O'Connell et al. 1994). In this case of two-site exchange across the erythrocyte membrane, these elements will form the 2×2 rate matrix R (Potts and Kuchel 1992; Gabel et al. 1997; Bulliman et al. 1989; Szekely et al. 2006) Eq. (9):

$$\boldsymbol{R} = \begin{bmatrix} \frac{1}{T_{1_A}} + k_A & -k_B \\ -k_A & \frac{1}{T_{1_B}} + k_B \end{bmatrix} \tag{9}$$

The linear equations of the lines with negative gradient will correspond to the first-order influx and efflux rate constants, whilst those with positive slope give the sum of the longitudinal relaxation rate constants of the I and E peaks

and the exchange rate constants (Bulliman et al. 1989; Perrin and Engler 1990).

The same principles apply to the analysis of the 2D EXSY data as that of the 1D Selective Inversion although the application is slightly different. Whilst a range of mixing times is still required, the longer acquisition time of the 2D EXSY imposes some restrictions on the number of mixing times used and therefore it is usual to use fewer mixing times than with the 1D equivalent. A 2D EXSY experiment is performed for each mixing time; one of these mixing times used must be 0 (Johnston et al. 1986; O'Connell et al. 1994; Gabel et al. 1997; Perrin and Dwyer 1999).

The matrix methods differ in that the matrices $M_t(\mathbf{M}_{t_m} - \mathbf{M}_{equi})$ and $M_0(\mathbf{M}_{t_m=0} - \mathbf{M}_{equi})$ of [4] are produced directly from the volumes of cross peaks and diagonal peaks of the of the spectra at each mixing time ($M_t$), including when $t_m = 0$ ($M_0$) (O'Connell et al. 1994; Johnston et al. 1986).

If:

$$\left(\mathbf{M}_t\mathbf{M}_0^{-1}\right) = \mathbf{A} = e^{-\mathbf{R}t} \tag{10}$$

then:

$$-\mathbf{R} = \frac{1}{t_m}\ln \mathbf{A} \tag{11}$$

or, from (7):

$$-\mathbf{R} = \frac{1}{t_m}\mathbf{X}(\ln \mathbf{\Lambda})\mathbf{X}^{-1} \tag{12}$$

where X is the square matrix of eigenvectors of A, $X^{-1}$ is its inverse, and ln Λ is the diagonal eigenvalue matrix (Jeener et al. 1979; Johnston et al. 1986; Macura and Ernst 1980). Clearly, this procedure is identical to that of the 1D Selective Inversion analysis, but with the alternative direct formation of matrix A from the 2D NMR data (Johnston et al. 1986):

$$\mathbf{A} = \begin{bmatrix} \frac{a_{AA}}{A_0} & \frac{a_{AB}}{B_0} \\ \frac{a_{BA}}{A_0} & \frac{a_{BB}}{B_0} \end{bmatrix} \tag{13}$$

where $a_{AA}$ and $a_{BB}$ are the diagonal peak amplitudes of site A and site B in an experiment with mixing; $a_{AB}$ and $a_{BA}$ are the cross peak amplitudes (showing exchange between site A and site B) in an experiment with mixing; and $A_0$ and $B_0$ are the diagonal peak amplitudes of site A and site B in an experiment without mixing ($t_m = 0$).

**Acknowledgements** ED thanks the Engineering and Physical Sciences Research Council for funding a PhD studentship. ED also thanks the Daphne Jackson Trust for a Fellowship funded by the Biotechnology and Biological Sciences Research Council and Royal Society of Chemistry. We thank the Medical Research Council for funding this research for JF. ED would also like to Dr Julie Wilson and Dr Meghan Halse, Department of Chemistry, University of York, Heslington, York, UK for advice.

**Author contributions** Project conception: JF; Experimental design: JF, ED; Sample preparation, data acquisition and data analysis: ED; Manuscript preparation: ED, JA.

**Compliance with ethical standards**

**Conflict of interest** The authors declare that they have no conflict of interest.

**Ethical approval** All procedures performed in studies involving human participants were in accordance with the ethical standards of the institutional and/or national research committee and with the 1964 Helsinki declaration and its later amendments or comparable ethical standards.



## References

Adiga U, D'Souza V, Kamath A, Mangalore N (2007) Antioxidant activity and lipid peroxidation in preeclampsia. J Chin Med Assoc 70:435–438

Bellon SF, Chen D, Johnston ER (1987) Quantitative 1D exchange spectrosocpy. J Magn Reson 73:168–173

Bremer J, Mendz GL, Moore WJ (1984) Skewed exchange spectroscopy. Two dimensional method for the measurement of cross relaxation in $^1$H NMR spectroscopy. J Am Chem Soc 106:4691–4696

Bulliman BT, Kuchel PW, Chapman BE (1989) "Overdetermined" one-dimensional NMR exchange analysis. A 1D counterpart of the 2D EXSY experiment. J Magn Reson, 82:131–138

Chapman BE, Kuchel PW (1990) Fluoride transmembrane exchange in human erythrocytes measured with $^{19}$F NMR. Eur Biophys J 19:41–45

Davey DA, MacGillivray I (1988) The classification and definition of the hypertensive diseases of pregnancy. Am J Obstet Gynecol 158:892–898

Davidge ST, Hubel CA, Brayden RD, Capeless EC, McLaughlin MK (1992) Sera antioxidant activity in uncomplicated and preeclamptic pregnancies. Obstet Gynecol, 79:897–901

Davies KJA (1987) Protein damage and degradation by oxygen radicals. J Biol Chem 262:9895–9901

El Hassan MA, Diamandis EP, Karumanchi SA, Shennan AH, Taylor RN (2015) Preeclampsia: an old disease with new tools for better diagnosis and risk management. Clin Chem 61:694

Engler RE, Johnston ER, Wade CG (1988) Dynamic parameters from nonselectively generated 1D exchange spectra. J Magn Reson 77:377–381

Esterbaur H, Schaur RJ, Zollner H (1991) Chemistry and biochemistry of 4-hydroxynonenal, malondialdehyde and related aldehydes. Free Radic Biol Med 11:81–128

Ethordevic NZ, Babic GM, Markovic SD, Ognjanovic BI, Stajn AS, Zikic RV, Saicic ZS (2008) Oxidative stress and changes in

antioxidant defense system in erythrocytes of preeclampsia in women. Reprod Toxicol 25:213–218
Forsén S, Hoffman RA (1963) Study of moderately rapid chemical exchange reactions by means of nuclear magnetic double resonance. J Chem Phys 39:2892–2901
Gabel SA, O'Connell TM, Murphy E, London RE (1997) Inhibition of glucose transport in human red blood cells by adenosine antagonists. Am J Phys, 272 (Cell Physiol. 41), C1415–1419
Grassi M, Mann BE, Pickup BT, Spencer CM (1986) The Determination of individual rates from magnetization-transfer measurements. J Magn Reson 69:92–99
Harsem NK, Braekke K, Staff AC (2006) Augmented oxidative stress as well as antioxidant capacity in maternal circulation in preeclampsia. Eur J Obstet Gynecol Reproduct Bioly 128:209–215
Hernandez-Garcia L, Lewis DP, Moffat B, Branch CA (2007) Magnetization transfer effects on the efficiency of flow-driven adiabatic fast passge inversion of arterial blood flow. NMR Biomed 20:733–742
Howlander ZH, Kabir Y, Khan TA, Islam R, Begum F, Huffman FG (2007) Plasma lipid profile, lipid peroxidation and antioxidant status in preeclampsia and uncomplicated pregnancies in Bangladesh. J Med Sci 7:1276–1282
Hubel CA (1999) Oxidative Stress in the Pathogenesis of Preeclampsia. Proc Soc Exp Biol Med 222:222–235
Hubel CA, Roberts JM, Taylor RN, Musci TJ, Rogers GM, McLaughlin MK (1989) Lipid peroxidation in pregnancy: new perspectives in preeclampsia. Am J Obstet Gynecol 161:1025–1034
Jeener J, Meier BH, Bachmann P, Ernst RR (1979) Investigation of exchange processes by 2-dimensional NMR-spectroscopy. J Chem Phys 71:4546–4553
Joffe GM, Esterlitz JR, Levine RJ, Clemens JD, Ewell MG, Sibai BM, Catalano PM (1998) The relationship between abnormal glucose tolerance and hypertensive disorders of pregnancy in healthy nulliparous women. Am J Obstet Gynecol 179:1032–1037
Johnston ER, Dellwo MJ, Hendrix J (1986) Quantitative 2D exchange spectroscopy using time-proportional phase incrementation. J Magn Reson 66:399–409
Jones DP (2008) Radical-free biology of oxidative stress. Am J Cell Phys 295:C849–C868
Kaur G, Mishra S, Sehgal A, Prasad R (2008) Alterations in lipid peroxidataion and antioxidant status in pregnancy with preeclampsia. Mol Cell Biochem 313:37–44
Kirk K, Kuchel PW (1985) Red cell volume changes monitored by a new $^{31}$P NMR procedure. J Magn Reson 62:568–572
Kirk K, Kuchel PW (1986) Equilibrium exchange of dimethyl methylphosphonate across the human red cell mebrane measured using NMR spin transfer. J Magn Reson 68:311–318
Kirk K, Kuchel PW (1988) Characterization of transmembrane chemical shift differences in the $^{31}$P NMR spectra of various phosphoryl compounds added to erythrocyte suspensions. BioChemistry 27:8795–8802
Kuchel PW, Chapman BE, Potts JR (1987) Glucose transporter in human erythrocytes measure using 13 C NMR spin transfer. FEBS Letters, 219, 5–10
Kuchel PW, Bulliman BT, Chapman BE, Mendz GL (1988) Variances of rate constants estimated from 2D NMR exchange spectra. J Magn Reson 76:136–142
Kumru S, Godekmerdan A, Kutlu S, Ozcan Z (2006) Correlation of maternal serum high-sensitive C-reactive protein levels with biochemical and clinical parameters in preeclampsia. Eur J Obstet Gynecol Reproduct Biol 124:164–167
London RE, Gabel SA (1995) Fluorine-19 NMR studes of glucosyl fluoride transport in human erythrocytes. Biophys J 69:1814–1818
Macura S, Ernst RR (1980) Elucidation of cross relaxation in liquids by two-dimensional N.M.R. spectroscopy. Mol Physs 41:95–117
May JM (1998) Ascorbate function and metabolism in the human erythrocyte. Front Biosci 2:d1–10
McConnell HM (1958) Reaction rates By nuclear magnetic resonance. J Chem Phys 28:430–431
Mehendale S, Kilari A, Dangat K, Taralekar V, Mahadik S, Joshi S (2008) Fatty acids, antioxidants, and oxidative stress in preeclampsia. Int J Gynecol Obst 100:234–238
Meier BH, Ernst RR (1979) Elucidation of chemical exchange networks by two-dimensional NMR spectroscopy: the heptamethylbenzenonium ion. J Am Chem Soc 101:6441–6442
Mohan KS, Venkataramana G (2007) Status of lipid peroxidation, glutathione, ascorbic acid, vitamin E and antioxidant enzymes in patients with pregnancy-induced hypertension. Indian J Phys Pharmacol 51:284–288
Montelione GT, Wagner G (1989) 2D chemical exchange NMR spectroscopy by proton-detected heteronuclear correlation. J Am Chem Soc 111:3096–3098
Muhandiram DR, McClung RED (1987) Multisite magnetization transfer experiments. J Magn Reson 71:187–192
Negre-Salvayre A, Coatrieux C, Ingueneau C, Salvayre R (2008) Advanced lipid peroxidation end products in oxidative damage to proteins. Potential role in diseases and therapeutic prospects for the inhibitors. Br J Pharmacol 153:6–20
O'Connell TM, Gabel SA, London RE (1994) Anomeric dependence of fluorodeoxyglucose transport in human erythrocytes. BioChemistry 33:10985–10992
Pallotta V, Gevi F, D'Alessandro A, Zolla L (2014) Storing red blood cells with vitamin C and N-acetylcysteine prevents oxidative stress-related lesions: a metabolomics overview. Blood Transfus 12:367–387
Parra-Cordero M, Sepúlveda-Martínez A, Preisler J, Pastén J, Soto-Chacón E, Valdés E, Rencoret G (2014) Role of the glucose tolerance test as a predictor of preeclampsia. Gynecol Obstet Invest 78:130–135
Patil SB, Kodliwadmath MV, Kodliwadmath SM (2007) Role of lipid peroxidation and enzymatic antioxidants in pregnancy-induced hypertension. Clin Exp Obstet Gynecol 34:239–241
Perrin CL, Dwyer TJ (1999) Application of two-dimensional NMR to kinetics of chemical exchange. Chem Rev 90:936–967
Perrin CL, Engler RE (1990) Weighted linear-least-squares analysis of EXSY data from multiple 1D selective inversion experiments. J Magn Reson 90:363–369
Perrin CL, Gipe RK (1984) Multisite kinetics by quantitative two-dimensional NMR. J Am Chem Soc 106:4036–4038
Poston L, Briley AL, Seed PT, Kelly FJ, Shennan AH (2006) Vitamin C and vitamin E in pregnant women at risk for pre-eclampsia (VIP trial): randomised placebo-controlled trial. Lancet 367:1145–1154
Potts JR, Kuchel PW (1992) Anomeric preference of fluoroglucose exchange across human red-cell membranes. Biochem J 281:753–759
Potts JR, Kirk K, Kuchel PW (1989) Characterization of the transport of the nonelectrolyte dimethyl methylphosphonate across the red cell membrane. NMR Biomed 1:198–204
Potts JR, Hounslow AM, Kuchel PW (1990) Exchange of fluorinated glucose across the red-cell membrane measured by 19F-n.m.r. magnetization transfer. Biochem J 266:925–928
Raftos JE, Bulliman BT, Kuchel PW (1990) Evaluation of an electrochemical model of erythrocyte pH buffering using $^{31}$P nuclear magnetic resonance data. J Gen Physiol 95:1183–1204
Raijmakers MTM, Roes EM, Poston L, Steegers EAP, Peters WHM (2008) The transient increase of oxidative stress during normal pregnancy is higher and persists after delivery in woman with pre-eclampsia. Eur J Obstet Gynecol Reproduct Biol 138:39–44

Riley GJ, Taylor NF (1973) The interaction of 3-deoxy-3-fluoro-D-glucose with the hexose-transport system of the human erythrocyte. Biochem J 135:773–777

Robinson G, Kuchel PW, Chapman BE, Doddrell DM, Irving MG (1985) A simple procedure for selective inversion of NMR resonances for spin transfer enzyme kinetic measurements. J Magn Reson 64:314–319

Roche M, Rondeau P, Singh NR, Tarnus E, Bourdon E (2008) The antioxidant properties of serum albumin. FEBS Lett 582:1783–1787

Salvi A, Carrupt P-A, Tillement J-P, Testa B (2001) Structural damage to proteins caused by free radicals: assessment, protection by antioxidants, and influence of protein binding. Biochem Pharmacol 61:1237–1242

Shoji H, Koletzko B (2007) Oxidative stress and antioxidant protection in the perinatal period. Curr Opin Clin Nutr Metab Care 10:324–328

Shoji H, Yamashiro Y, Koletzko B (2008) Oxidative stress and antioxidants in the perinatal period. Oxid Stress Dis 23:71–92

Stadtman ER (1993) Oxidation of free amino acids and amino acid residues in proetins by radiolysis and by metal-catalyzed reactions. Annu Rev Biochem 62:797–821

Szekely D, Chapman BE, Bubb WA, Kuchel PW (2006) Rapid Exchange of fluoroethylamine via the rhesus complex in human erythrocytes: 19F NMR magnetization transfer analysis showing competition by ammonia and ammonia analogues. BioChemistry 45:9354–9361

Turner E, Brewster JA, Simpson NAB, Walker JJ, Fisher J (2007) Plasma from women with preeclampsia has a low lipid and ketone body content—A nuclear magnetic resonance study. Hypertens Pregnancy 26:329–342

Turner E, Brewster JA, Simpson NAB, Walker JJ, Fisher J (2008) Aromatic amino acid biomarkers of preeclampsia—A nuclear magnetic resonance investigation. Hypertens Pregnancy 27:225–235

Turner E, Brewster JA, Simpson NAB, Walker JJ, Fisher J (2009) Imidazole-based erythrocyte markers of oxidative stress in preeclampsia—An NMR investigation. Reproduct Sci 16:1040–1051

Xu AS-L, Potts JR, Kuchel PW (1991) The phenomenon of separate Intra- and extracellular resonances of difluorophosphate in $^{31}P$ and $^{19}F$ NMR spectra of erythrocytes. Magn Reson Med 18:193–198